Journal of Ceramic Processing Research. Vol. 9, No. 2, pp. 184~188 (2008)

J O U R N A L O F
Ceramic Processing Research

Two-dimensional simulation of silica gel drying using computational fluid dynamics

Chi-Young Jung[a], Jong-Ryul Kim[b] and Sung-Chul Yi[a,*]
[a]*Department of Chemical Engineering, Hanyang University, Seoul 133-791, Korea*
[b]*Research Institute, ENE System Co. Ltd., Seoul 137-073, Korea*

In this study, a two-dimensional, mathematical model for the analysis of the mass and heat transfer of moisture and water vapor in a humid-air dryer was developed using a commercially-available computational fluid dynamics code, Fluent®. A thin-layer drying approach of drying kinetics for a general silica gel in computational fluid dynamics modeling was included in this work. Simulations were carried out for the top-tray position of the dryer and two different cases for structural designs: CASE 1 and CASE 2. By using an evaporation model, coupled with a moisture diffusion model, it was possible to calculate the moisture content and water vapor distribution inside the dryer. Consequently, using the proposed model, it was possible to analyze the relation between flow velocity and drying rate and estimate the optimal design of the dryer, CASE 2.

Key words: Drying, Humid Air, Cfd, Model.

Introduction

Drying is a mass transfer process resulting in the removal of water moisture or moisture from another solvent, by evaporation from a solid, semi-solid or liquid (hereafter product) to end in a solid state [1]. It is an important process in the fine chemicals, food, pharmaceutical products industries, etc [2]. Also, in some areas of synthetic chemistry, drying is a required process to obtain target material such as for aero-gel synthesis [3].

Pesaran and Mills [4, 5] studied the moisture transport in a thin silica gel packed-bed system with an experimental study and an analytical model. San and Jiang [6] tested a two-column packed-bed desiccant dehumidification system and analytical modeling was also conducted. A drying model which may be used for both hygroscopic and non-hygroscopic materials was developed by Chen and Pei [7]. But none of these models considered thin-layer drying. The thin-layer drying model describes the combined mechanisms of heat and mass transport phenomena and enables an investigation of the influences that certain process variables exert on moisture removal processes.

In the present study, a two-dimensional mathematical model for a drying process is developed, which considers internal moisture diffusion, evaporation, and related heat transfer using a thin-layer drying model. The drying rate constant, which is a key parameter in our model, was obtained as a function of humidity, velocity, and temperature of dry air from the literature. A finite volume method [11, 12] is used to calculate the differential equations numerically.

*Corresponding author:
Tel : 82-2-2220-0481
Fax: 82-2-2298-5147
E-mail: scyi@hanyang.ac.kr

Mathematical Model

In our present research, as illustrated in Fig. 1. a two-dimensional humid-air tray dryer system was considered as the computational domain. The left figure, CASE 1, is an example figure of the dryer. And the right figure, CASE 2, is a modified figure in order to obtain an enhanced velocity profile. For numerical convenience, all simulations were performed with a two-dimensional mathematical model, only considering the drying room with twenty-six trays. The modeled region is separated into three regions: silica gel, dry air, and the interface between solid and air.

Model assumptions

To reduce complexity in the numerical calculation of liquid-gaseous two-phase situation, the proposed model includes the following assumptions:

1) Ideal gas mixture for gaseous fluid.
2) Turbulent flow.
3) Non-isothermal model.
4) Unsteady-state model.
5) No penetration of gaseous-fluid into the silica gel.
6) Silica gel is uniform in size during drying.

Governing equations

As stated in assumption 3, liquid-moisture exists only inside the silica particles. In our study, a single-domain model formation was used for the governing equations, which are valid for all the sub-regions used. Therefore, no interfacial conditions are used at interfaces between the components of the cell. Under the foregoing model assumptions, the governing equations can be written as below:

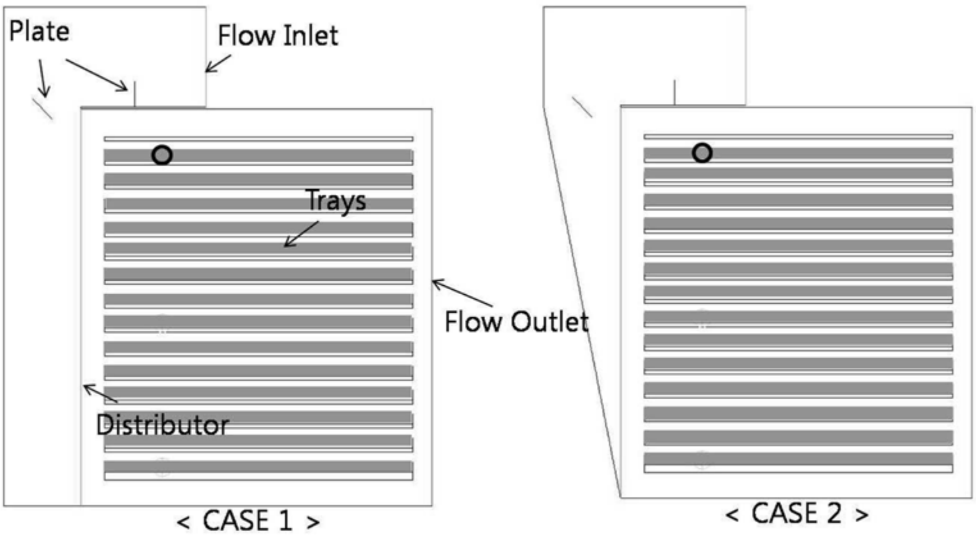

Fig. 1. Schematic of a two-dimensional humid-air dryer: CASE 1 and CASE 2.

$$\frac{\partial \rho_g}{\partial t} + \nabla \cdot (\rho_g u) = 0 \tag{1}$$

$$\frac{\partial \rho_g u}{\partial t} + \nabla \cdot (\rho_g u u) = -\nabla P + \nabla \cdot (\mu_g \nabla u) \tag{2}$$

$$\frac{\partial C_i}{\partial t} + \nabla \cdot (u C_i) = \nabla \cdot (D_i^{eff} \nabla C_i) + S_i \tag{3}$$

$$\frac{\partial (\rho_g C_p T)}{\partial t} + \nabla \cdot (\rho_g u C_p T) = \nabla \cdot (k^{eff} \nabla T) + S_T \tag{4}$$

The mass conservation equation is shown as Eq. (1), where ρ_g is the density of the gas mixture. The momentum conservation equation is shown as Eq. (2), where μ_g is the viscosity of the gas mixture. Here, we assumed a constant value for density and viscosity of the gas mixture (See Table 1).

The species conservation equation is shown as Eq. (3), where D_i^{eff} is the effective diffusion coefficient of species i (e.g. air and water vapor) and is defined as a function of temperature and pressure [8] by the following equation:

$$D_i^{eff} = D_i \left(\frac{T}{T_0}\right)^{3/2} \left(\frac{P_0}{P}\right) \tag{5}$$

Transport properties for species are summarized in Table 1.

The source/sink terms, S_k, S_T, in Eq. (3) and (4) over three regions of the domain are given in Table 2.

Moisture diffusion and evaporation

When a wet silica gel is exposed to thermal drying, the following processes occur simultaneously [1]:

1. Transfer of energy from the surrounding environment to evaporate the surface moisture;
2. Transfer of internal moisture to the surface of the solid and its subsequent evaporation.

As evaporation takes place at the surface of silica gel particles, internal moisture migrates to the surfaces of the particles due to diffusion, capillary flow, and an internal pressure gradient. In this study, the internal pressure gradient effect was ignored and diffusion and capillary flow were combined into an effective diffusion. The effective diffusion coefficient is obtained by considering the activation energy for diffusion as a function of material moisture content [4, 5]:

$$D_m = D_{m,0} \exp((E_0 - E_1 X)/T) \tag{6}$$

where $E_0 = 2450\text{K}$, $E_1 = 1400\text{K/(kg/kg db)}$.

To solve the moisture specie conservation equation, a thin-layer equation is defined to estimate the changes in moisture content as time flows. The thin-layer drying

Table 1. Transport properties

Property	Value
H_2O diffusivity in the dryer, D_w^0	1.10×10^{-4} m^2/s
AIR diffusivity in the dryer, D_a^0	3.20×10^{-5} m^2/s
X diffusivity in the silica gel, $D_{m,o}$	5.71×10^{-7} m^2/s
Density of silica gel, ρ_{sg}	1650 kg/m^3
Density of gas mixture, ρ_g	1.225 kg/m^3
Viscosity of gas mixture, μ_g	1.7894×10^{-5} kg/m · s

Table 2. Source/sink terms for species and energy conservation equations for individual regions

	H_2O-vapor	Moisture content	Temperature
Air	$S_w = 0$	$S_m = 0$	$S_T = 0$
Interface	$S_w = K(X-X_{eq})\rho_{sg}/M_w$	$S_m = -K(X-X_{eq})$	$S_T = -H_m \times M_w \times S_w$
Silica Gel	$= 0$	$S_m = 0$	$S_T = 0$

equation [1] has the following form:

$$-\frac{dX}{dt} = K(X - X_{eq}) \tag{7}$$

where is the drying rate constant and is the equilibrium moisture content.

Transport properties, such as moisture diffusivity, thermal conductivity, interfacial heat and mass transport coefficients, can completely describe the drying kinetics. The drying rate constant is a concept introduced from eqn. (7), which is a combination of these transport properties. The drying rate constant, K, is the most appropriate variable for the purpose of designing and optimizing any type of drying system, in which a large number of iterative model calculations are needed.

The equilibrium moisture content is a function of the temperature and humidity conditions [9]. For silica gel, the equilibrium moisture content is calculated as below [10]:

$$X_{eq} = 0.25 \times (h_a)^{0.6} \tag{8}$$

Boundary conditions

Eq. (1) through (4) form the complete set of governing equations for the conventional mathematical model. Boundary conditions are only required at the external boundaries due to the single-domain model approach used in this model. The no-flux conditions are applied for mass, momentum, species and energy conservation equations at all boundaries except for the inlet and outlet of the dryer. At the inlet, the inlet velocity, temperature and the species concentrations are specified in Table 3. The species concentrations of the inlet are determined by the relative humidity at a specified temperature.

Numerical Method

In this study, mathematical modeling and simulation of a two-dimensional tray dryer for two different cases were performed with a commercially available CFD code, FLUENT. All governing equations except the momentum conservation equation were solved using User Defined Functions (UDFs).

The UDFs are, in general, C routines programmed by the user linked to the solver to perform certain operations such as 1) initializations, 2) specification of boundary conditions, 3) specification of material properties, 4) adapting source terms into each governing equation, and 5) post-processing and reporting. Here, an evaporation UDF add-on module was developed to analyze and perform an optimal design of the dryer.

By grid dependency examination, approximately 50,000 computational cells were found to be adequate and used for all simulations. About 50 iterations were taken for each time step, while the time step size was set at 10 seconds. The maximum flow time was 5 hours for all cases.

Results and Discussion

Model prediction

The drying kinetics are estimated with the change of solid moisture content and temperature with respect to time elapsed. The so-called drying curves, which describe moisture content of the silica gel particles with time are shown in Fig. 2. The curves are taken at the circled position in the top tray from Fig. 1. As shown in here, the moisture content decreases linearly as time flows. Then the drying rate decreases, approaching the equilibrium moisture contents in a form of parabolic curve.

Fig. 3. shows variation of the drying rate constant with time elapsed. Initially, the drying rate constant increases linearly as time flows. However, around 60-80 minutes, linear lines turn into curves. With further elapsed time the rate gradually decreases with moisture content decrement.

Comparison between the CASE 1 and CASE 2

Fig. 4 and 5 show velocity vectors of the considered drying systems: CASE 1 and CASE 2. As shown in Fig. 4, velocity distributions through the trays are not uniform. The "Dead Zone", in which flow velocities are under 0.3 ms^{-1} is generated near the left bottom side of the dryer. Also, the most bottom path has a flow

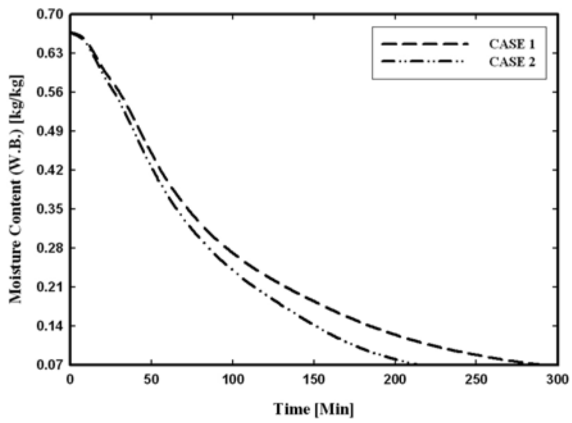

Fig. 2. Average drying kinetic curves at the top tray with 70 °C inlet air condition: CASE 1 and CASE 2.

Table 3. Boundary/initial conditions

	Momentum	Temperature	Pressure	X	C_w
Dryer inlet	4 m/s	70 °C	-	0	1.550×10^{-3} mol/m^3
Dryer outlet	-	-	101325 Pa	-	-
Initial Conditions	X_{ini}	0.66	-	-	-

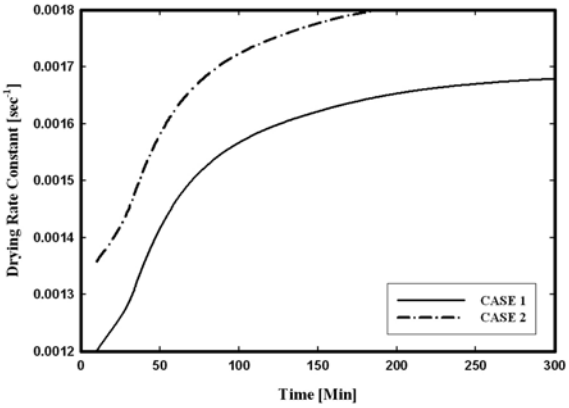

Fig. 3. Average drying kinetic curves at the top tray with 70 °C inlet air condition: CASE 1 and CASE 2.

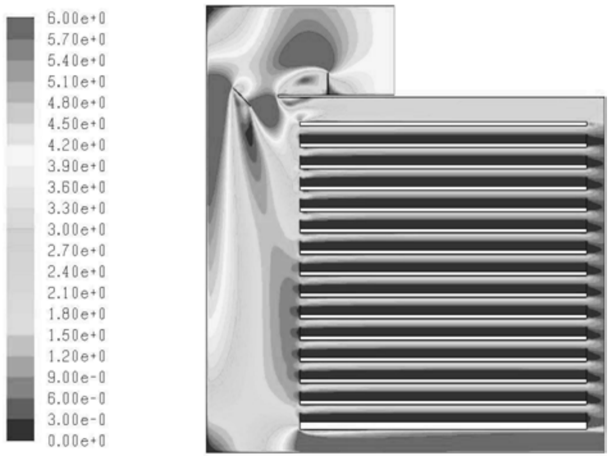

Fig. 4. Velocity contour in the CASE 1 dryer.

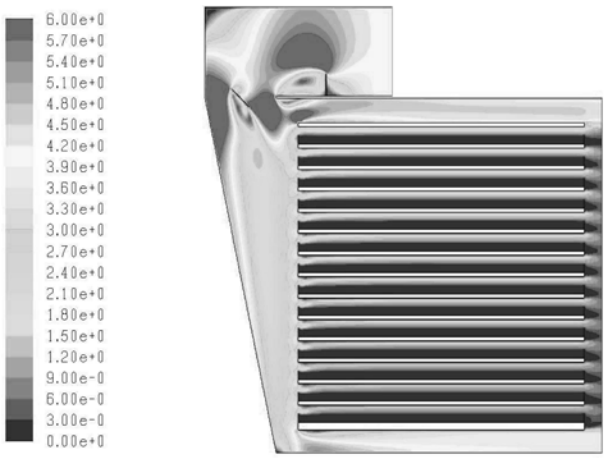

Fig. 5. Velocity contour in the CASE 2 dryer.

velocity above 5 ms^{-1}. In other tray inlets, an average velocity of 1.5 ms^{-1} is gained here. As the drying rate constant is a function of flow velocity, the CASE 1 dryer has a structural weak point from this viewpoint. Therefore, a flow distribution from the bottom path to other trays is required.

In Fig. 5, velocity distributions through the trays are more uniform than for CASE 1. Moreover, in the tray inlets, the average velocity is above 2.5 ms^{-1}. As the flow velocity of the CASE 2 is approximately 1.66 times faster than for CASE 1, the drying rate is 1.16 times faster from the thin-layer equation (eqn. (7)).

Conclusions

A two dimensional, non-isothermal and transient model for a humid-air drying system was developed based on a moisture diffusion and evaporation model. With the module developed using user-defined-functions (UDFs) included in FLUENT, it was possible to investigate the flow velocity effect on the drying rate. From a comparison of drying kinetic curves between CASE 1 and CASE 2, the results indicate that the CASE 2 dryer has an improved drying performance due to enhanced air velocity, which directly leads to a drying rate constant increment.

Although the model developed in this study is simple, velocity, relative humidity, and inlet temperature effects can be incorporated into the model, which enhances the capabilities for design engineers to analyze and optimize a humid-air dryer.

Acknowledgements

The authors are grateful for the financial support through grant no. 2005-E-ID11-P-14 by Energy Saving Technology Development Program from the Korea Energy Management Corporation (KEMCO).

Nomenclature

List of symbols

C	molar concentration [mol/m^3]
C_p	heat capacity [J/kg · K]
D	mass diffusion coefficient [m^2/s]
H	latent heat of evaporation [J/kg]
h	relative humidity
K	drying rate constant [sec^{-1}]
k	thermal conductivity [W/m · K]
M	molecular weight [kg/mol]
P	pressure [pa]
S	Source/sink term
t	time [sec]
T	temperature [K]
u	velocity vector [m/s]
X	moisture content [kg/kg]

Greek letters

ρ	density [kg/m^3]
μ	viscosity [kg/m · s]

Superscripts

eff	effective

Subscripts

a	air
eq	equilibrium
g	gas mixture
i	species
ini	initial
m	moisture
o	STP condition
sg	silica gel
t	temperature
w	H_2O vapor

References

1. Arun S. Mujumdar, “Handbook of Industrial Drying”, Vol. 1, Marcel Dekker Inc., New York (1995).
2. A.H. Zahed, J.X. Zhu J.R. Grace, Drying Technology, 13 (1995) 1-13.
3. W.I. Kim and I.K. Hong, J. Ind. Eng. Chem. 9[6] (2003) 728-734.
4. A.A. Pesaran and A.F. Mills, Int. J. Heat Mass Transfer 30[6] (1987) 1037-1050.
5. A.A. Pesaran and A.F. Mills, Int. J. Heat Mass Transfer 30[6] (1987) 1051-1060.
6. J.Y. San and G.D. Jiang, Int. J. Heat Mass Transfer 37[8] (1994) 1173-1179.
7. P. Chen and D.C.T. Pei, Int. J. Heat Mass Transfer 32[2] (1989) 297-310.
8. R. B. Bird, W. E. Stewart and E. N. Lightfoot, Transport Phenomena, John Wiley, New York (1960).
9. A.S. Mujumdar and S. Davahastin, “Handbook of fluidization and fluid-particle systems”, Marcel Dekker Inc., New York (2003).
10. Y.S. Park, H.N. Shin, D.H. Lee, D.J. Kim, J.H. Kim, Y.K. Lee, S.J. Sim and K.B. Choi, Korean J. Chem. Eng. 20[6] (2003) 1170-1175.
11. S.-V. Patankar, Numerical Heat Transfer and Fluid Flow, Hemisphere Publishing Corporation (1980).
12. Fluent 6.3 User’s Guide, Fluent Inc., NH, U.